Control of the AtMAP65-1 interaction with microtubules through the cell cycle

Andrei P. Smertenko[1,*], Hsin-Yu Chang[1,*], Seiji Sonobe[2], Stepan I. Fenyk[1], Magdalena Weingartner[3], Laci Bögre[3] and Patrick J. Hussey[1,‡]

[1]The Integrative Cell Biology Laboratory, School of Biological and Biomedical Sciences, University of Durham, South Road, Durham, DH1 3LE, UK
[2]Himeji Institute of Technology, Faculty of Science, Hyogo, Japan
[3]School of Biological and Biomedical Sciences, Royal Holloway, University of London, Egham, TW20 0EX, UK

*These authors contributed equally to this work
‡Author for correspondence (e-mail: p.j.hussey@durham.ac.uk)

Accepted 17 May 2006
Journal of Cell Science 119, 3227-3237 Published by The Company of Biologists 2006
doi:10.1242/jcs.03051

Summary

Cell division depends on the fine control of both microtubule dynamics and microtubule organisation. The microtubule bundling protein MAP65 is a 'midzone MAP' essential for the integrity of the anaphase spindle and cell division. *Arabidopsis thaliana* MAP65-1 (AtMAP65-1) binds and bundles microtubules by forming 25 nm cross-bridges. Moreover, as AtMAP65-1 bundles microtubules in interphase, anaphase and telophase but does not bind microtubules in prophase or metaphase, its activity through the cell cycle must be under tight control. Here we show that AtMAP65-1 is hyperphosphorylated during prometaphase and metaphase and that CDK and MAPK are involved in this phosphorylation. This phosphorylation inhibits AtMAP65-1 activity. Expression of non-phosphorylatable AtMAP65-1 has a negative effect on mitotic progression resulting in excessive accumulation of microtubules in the metaphase spindle midzone causing a delay in mitosis. We conclude that normal metaphase spindle organisation and the transition to anaphase is dependent on inactivation of AtMAP65-1.

Key words: Microtubule-associated protein, MAP-65, Division midzone, Regulation

Introduction

Microtubule organisation undergoes dramatic spatial rearrangement during the cell cycle and in particular at the G2/M phase transition and throughout mitosis. The establishment of mitotic spindle polarity and the correct positioning of the chromosomes on the metaphase plate are accompanied by increased microtubule dynamics (Saxton et al., 1984; Verde et al., 1990; Hush et al., 1994). This increase in dynamics is attributed mainly to the coordinated activity of MAPs acting at the growing ends of microtubules (Kline-Smith and Walczack, 2004). From anaphase onwards the maintenance of the microtubule structure between the separating chromosomes (the central spindle) is coordinated by a group of microtubule-associated proteins known as the 'midzone MAPs' so called because of their localisation at the central spindle (Glotzer, 2005). In mammals, two classes of microtubule-binding proteins are essential for the maintenance of the anaphase spindle midzone. The first class are kinesins, which include the microtubule plus-end directed BimC-like kinesin, the microtubule minus-end directed C-terminal motor domain Kar3 kinesin and the microtubule bundling MKLP1/CHO1 kinesin. The second class includes non-motor proteins PRC1 and Mast-Orbit. PRC1 (and its homologues in other eukaryotes) is essential for cytokinesis and is important for the maintenance of the central spindle whereas the function of Mast-Orbit in this structure is still not understood (Pellman et al., 1995; Verni et al., 2004; Verbrugghe and White, 2004).

So far we know very little about the organisation of the central spindle in plants, and the components are just beginning to be identified (Otegui et al., 2005). The MAP65 family of proteins are PRC1 homologues and are important for central spindle organisation during plant cell division (Smertenko et al., 2000; Müller et al., 2004). MAP65 is one of the most abundant plant structural microtubule-associated proteins (Jiang and Sonobe, 1993), capable of microtubule bundling and producing 25 nm cross-bridges between microtubules (Jiang and Sonobe, 1993; Chan et al., 1999; Smertenko et al., 2004). In *Arabidopsis thaliana* MAP65 is encoded by a family of nine genes (Hussey et al., 2002). One of these, AtMAP65-1, belongs to a conserved group of plant MAP-65s which exhibits a cell cycle-dependent pattern of microtubule binding. AtMAP65-1 binds to a subset of microtubules in the interphase array and the preprophase band (PPB). However, as the PPB disassembles and the mitotic spindle starts to form, AtMAP65-1 becomes mainly cytoplasmic (Smertenko et al., 2004; Van Damme et al., 2004; Chang et al., 2005). As the chromosomes separate AtMAP65-1 is observed to associate with microtubules again in anaphase B, but its localisation is restricted to the midzone of the anaphase spindle and to the phragmoplast midzone during telophase (Smertenko et al., 2004; Chang et al., 2005). A similar localisation was reported for the AtMAP65-1 homologue in tobacco NtMAP65-1a (Smertenko et al., 2000) suggesting that both proteins have similar functions (Chang et al., 2005).

The principal activity of MAP65 is microtubule bundling. It has been proposed that AtMAP65-1 cross-bridges anti-parallel microtubules in the division midzone, which are involved in keeping two parts of the cytokinetic apparatus

together (Müller et al., 2004) until the development of a vesicular-tubular membrane network at the site of future cell plate formation. As the cell plate forms the microtubules crossing the division midzone disappear (Segui-Simarro et al., 2004) and MAP65 localisation at the division midzone fades (Chang et al., 2005). Phragmoplast microtubules depolymerise at the sites where the cell plate has been established and polymerise at the edges of the expanding cell plate to support the centrifugal expansion of the cell plate until it reaches the cell wall of the mother cell (Nishihama and Machida, 2001). The localisation of AtMAP65-1 at the midzone was detected at the edge of the expanding phragmoplast (Chang et al., 2005) where AtMAP65-1 most probably supports phragmoplast structure until the establishment of a vesicular-tubular membrane network. The role of MAP65 proteins in maintaining the integrity of the phragmoplast was demonstrated in the *A. thaliana* mutant, *pleiade*. Mutations in PLEIADE-AtMAP65-3 cause an increase of the 'clear zone' between the two halves of the phragmoplast and the accumulation of multinucleate cells due to a failure in cytokinesis (Müller et al., 2004).

AtMAP65-1 has a very dynamic interaction with microtubules in vivo and its microtubule-binding activity is regulated in a cell-cycle-dependent manner (Chang et al., 2005). The nature of this regulation is starting to be elucidated. Mao et al. (Mao et al., 2005) have recently shown that mutation of a potential CDK phosphorylation site at Ser503 can restore binding of AtMAP65-1 to microtubules in metaphase. Moreover, NtMAP65-1a activity is modulated by MAPK in cytokinesis. Phosphorylation of NtMAP65-1a by MAPK diminishes its microtubule bundling activity but not its binding ability and mutation of this single MAPK phosphorylation site delays cytokinesis (Sasabe et al., 2006).

In the work reported here we have examined whether phosphorylation is responsible for the control of AtMAP65-1 through the cell cycle and have found that AtMAP65-1 is hyperphosphorylated during prophase and metaphase. Phosphorylation inhibits AtMAP65-1 activity in a dose-dependent manner. Moreover, expression of non-phosphorylatable AtMAP65-1 has a negative effect on mitotic progression: accumulation of microtubules in the metaphase spindle midzone and a delay in the metaphase-anaphase transition.

Results

AtMAP65-1is hyperphosphorylated in prophase and metaphase

To investigate the possibility that MAP65 is controlled by reversible phosphorylation we established whether its phosphorylation state could be correlated with cell cycle stage. We used a synchronised cell culture and isolated total protein extracts from eleven sampling points through the cell cycle and used these to phosphorylate AtMAP65-1 in vitro (Fig. 1A). The results demonstrate that AtMAP65-1 is phosphorylated at all stages of the cell cycle but hyperphosphorylated at prophase and metaphase stages (Fig. 1Bi) when it does not bind microtubules (Smertenko et al., 2000; Smertenko et al., 2004; Van Damme et al., 2004; Chang et al., 2005). Each phosphorylation reaction had the same amount of recombinant AtMAP65-1 (Fig. 1Bii) and the same amount of total protein cell extract (Fig. 1Biii). Fractionation of total protein extracts from S-phase and M-phase cells by two-dimensional gel electrophoresis revealed an increase in the complexity of the constellation of AtMAP65-1 isoforms (Fig. 1C). Treatment with phosphatase minimised these constellations confirming

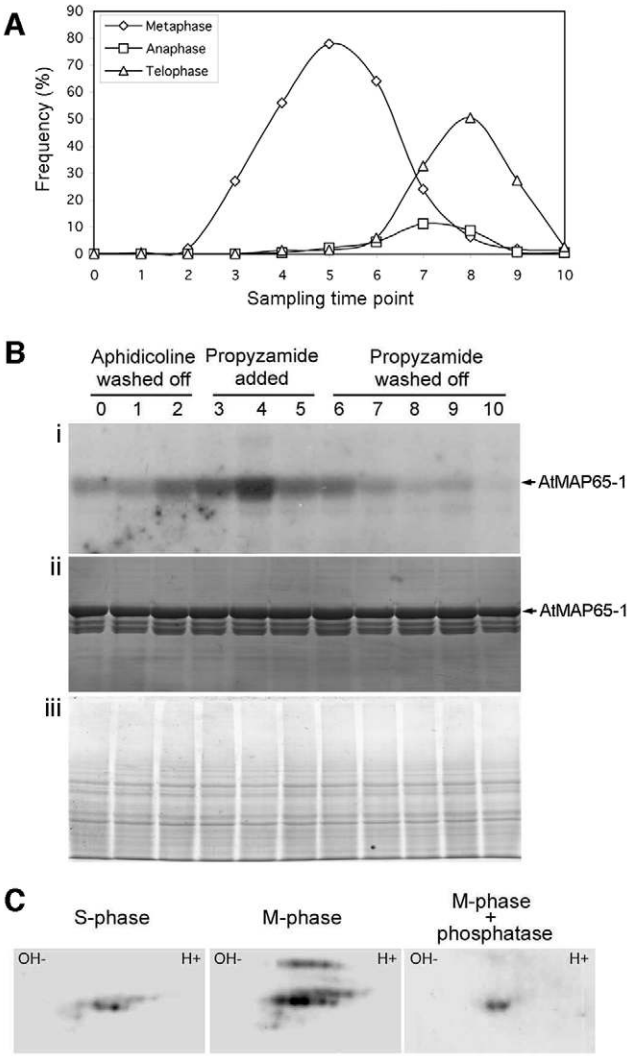

Fig. 1. Cell-cycle-dependent phosphorylation pattern of AtMAP65-1. (A) Cell cycle synchronisation. Graphs show the frequency of metaphase (open diamonds), anaphase (open squares) and telophase (open triangles) cells in the synchronised BY-2 cell culture. Eleven sampling points were analysed: points 0-2 were collected every two hours after aphidicolin was washed out, points 3-5 were collected every 2 hours during propyzamide treatment and points 6-10 were collected every 40 minutes after propyzamide was washed out with the exception that there was a 2-hour interval between points 9 and 10. (B) Autoradiogram (i) and Coomassie Blue-stained gel (ii) showing phosphorylation of AtMAP65-1 using the total protein extract from cells collected at sampling points 0-10 described in A (i). 5 μg of recombinant AtMAP65-1 was used in each assay. The Coomassie Blue-stained gel of the extracts used as kinase in (i) and (ii) is shown in (iii). (C) Two-dimensional SDS-PAGE immunoblots of total protein extracts from interphase cells (S-phase, sampling point 0), metaphase cells (M-phase, sampling point 4) and M-phase extract treated with phosphatase, probed with anti AtMAP65-1. The area of the membrane where AtMAP65-1 isoforms were detected is shown.

that AtMAP65-1 is phosphorylated during interphase and during metaphase in vivo. However, the complexity of the MAP65 constellation of spots in metaphase would indicate multiple phosphorylation events at this stage.

AtMAP65-1 is phosphorylated by several protein kinase pathways

To identify the kinase pathways responsible for the phosphorylation of MAP65 we repeated the AtMAP65-1 in vitro phosphorylation assays using M-phase extracts in the presence of specific and general protein kinase inhibitors (Fig. 2A). Whereas the general protein kinase inhibitors, staurosporine and K252a, knocked out all kinase activity, 6-dimethylaminopurine (DMAP) and the CDK-specific inhibitor olomoucine only partially inhibited kinase activity, suggesting that more than one protein kinase can phosphorylate AtMAP65-1. In vivo, both DMAP and olomoucine induced GFP:AtMAP65-1 to localise to the metaphase spindle microtubules within 10 minutes of treatment (Fig. 2D-F) indicating that the microtubule-binding activity of AtMAP65-1 is regulated by phosphorylation, possibly by several different pathways. Furthermore treatment of the GFP:AtMAP65-1 cell line with the phosphatase type 1 and 2A inhibitor okadaic acid progressively eliminated AtMAP65-1 binding to the microtubules at the midzone of the phragmoplast (Fig. 2G). Because inhibition of CDK activity by olomoucine induced the binding of AtMAP65-1 to microtubules we examined whether an increase in the activity of CDK would inhibit the binding of AtMAP65-1 to microtubules. We used a transgenic BY-2 cell line expressing a non-degradable mutant form of cyclin B1 under the control of a dexamethasone-inducible promoter. In this cell line activity of CDK is upregulated during telophase resulting in abnormal phragmoplast formation (Weingartner et al., 2004). However, MAP65-1 was still bound to phragmoplast microtubules in these cells after induction, suggesting that activity of CDK alone is not sufficient to abolish binding of MAP65-1 to microtubules (Fig. 2H).

Preparations of microtubule-associated proteins have been shown to have kinase activity (Fellous et al., 1994; Reszka et al., 1995). Bearing this is mind we generated a microtubule-associated protein (MAP) preparation from tissue culture cells and checked if it could phosphorylate AtMAP65-1. We used 1 μg of this MAP preparation and 1 μg of a total M-phase cell protein extract in the phosphorylation assays. The results show that the kinase activity in the MAP preparation is enriched compared to control, indicating that the MAP65 kinases associate in microtubule complexes (Fig. 2B). It has been reported that both CDKs and MAP kinases can be associated with microtubules (Fellous et al., 1994; Reszka et al., 1995). Using suc 1 beads, anti-cdc2a and 2b (cyclin-dependent

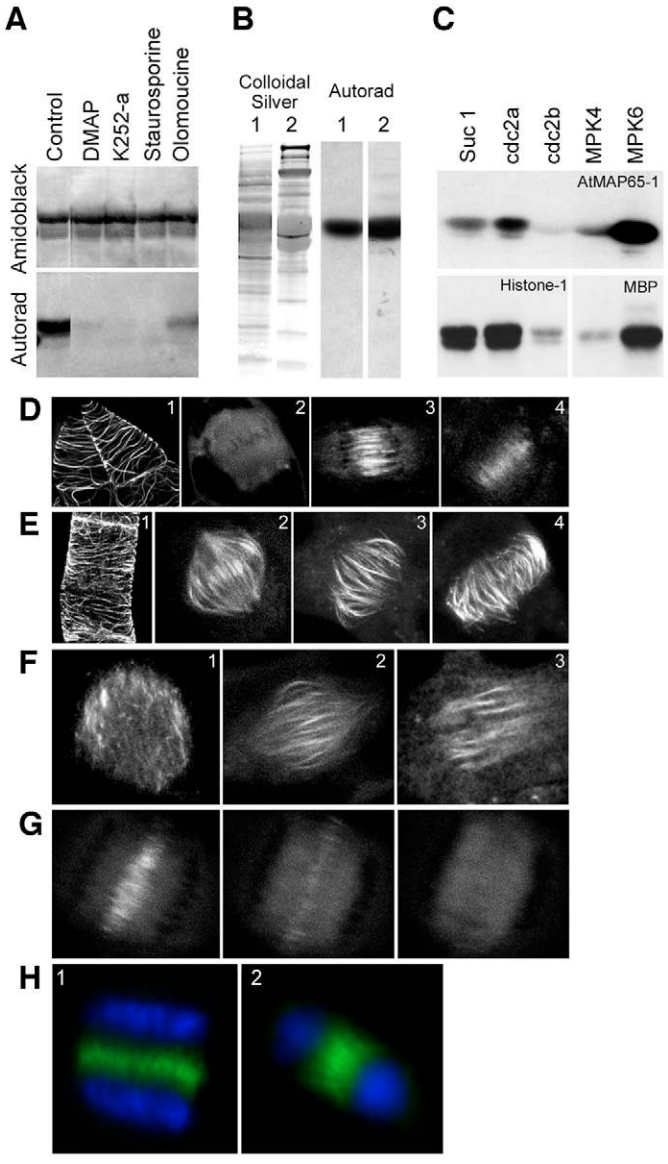

Fig. 2. Several protein kinases phosphorylate AtMAP65-1. (A) Effect of protein kinase inhibitors on AtMAP65-1 phosphorylation in vitro. Recombinant AtMAP65-1 was phosphorylated using M-phase extract (sampling point 4 as in Fig. 1A) without inhibitor (Control) or in the presence of 20 mM DMAP, 5 μM K252a, 5 μM staurosporine and 100 μM olomoucine. Each lane contained an equal amount of protein as shown by the amido-black staining. (B) AtMAP65-1 is phosphorylated by microtubule associating kinases. Colloidal silver staining and autoradiogram of phosphorylation assays using M-phase extract (lane 1) and a microtubule-associated protein preparation (lane 2). (C) AtMAP65-1 is phosphorylated by CDKs and MAPKs. Cyclin-dependent kinases were pulled down using pSuc1 bound beads, anti-cdc2a and anti-cdc2b. MAP kinases were immunoprecipitated with anti-MPK4 and anti-MPK6. Kinase activity was checked using histone 1 as a substrate for cyclin-dependent kinases and using myelin basic protein (MBP) as the substrate for MAP kinases. (D) Localisation of GFP:AtMAP65-1 in control cells. (Interphase (1), metaphase (2), anaphase (3) telophase (4). (E) Localisation of GFP:AtMAP65-1 in cells treated for 10 minutes with the general protein kinase inhibitor DMAP. Interphase (1), metaphase (2), anaphase (3) and telophase (4). (F) Localisation of GFP:AtMAP65-1 in cells treated for 10 minutes with the CDK inhibitor olomoucine. Prometaphase (1), metaphase (2 and 3). (G) Three consecutive movie frames (taken 2 minutes apart) of a cell treated with the phosphatase inhibitor okadaic acid. The images were recorded after 15 minutes of treatment. Note the GFP:AtMAP65-1 signal disappears and the phragmoplast does not expand in this time. (H) Localisation of AtMAP65-1 (green signal) and DNA (blue signal) in the phragmoplast of a BY-2 cell line harbouring a non-degradable form of cyclin B1 under the control of the dexamethasone-inducible promoter before induction (1) and after 16 hours induction with dexamethasone (2).

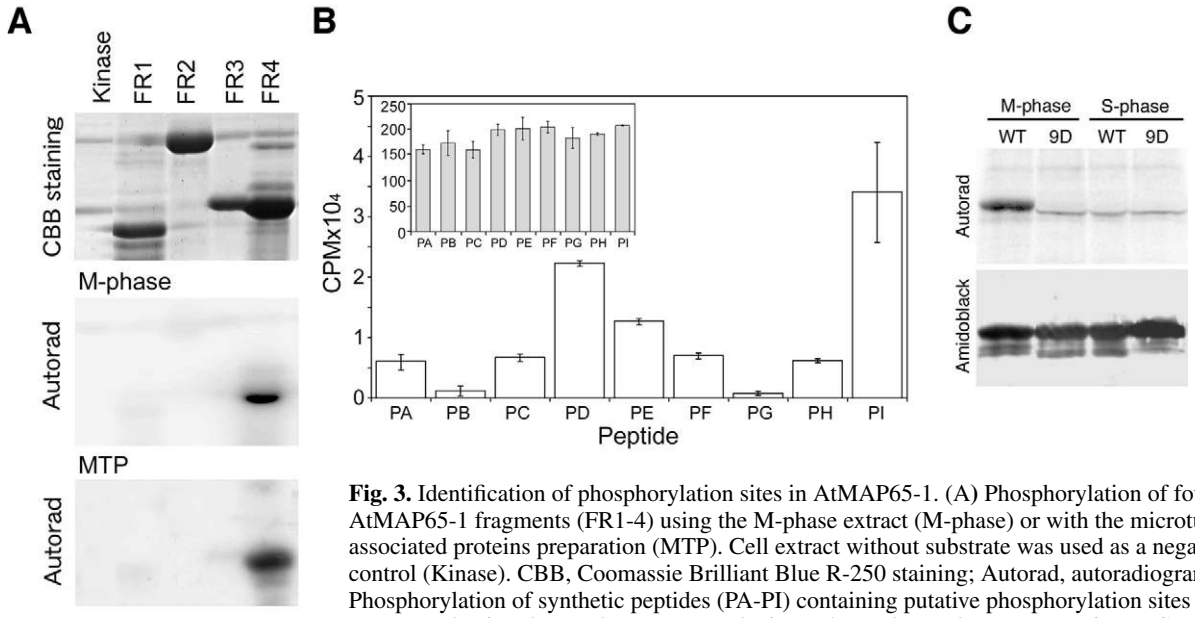

Fig. 3. Identification of phosphorylation sites in AtMAP65-1. (A) Phosphorylation of four AtMAP65-1 fragments (FR1-4) using the M-phase extract (M-phase) or with the microtubule-associated proteins preparation (MTP). Cell extract without substrate was used as a negative control (Kinase). CBB, Coomassie Brilliant Blue R-250 staining; Autorad, autoradiogram. (B) Phosphorylation of synthetic peptides (PA-PI) containing putative phosphorylation sites in Fragment 4 using the M-phase extract. The inset shows the total counts per minute (CPM) in the corresponding reaction mixtures. (C) Autoradiogram (Autorad) of the recombinant wild-type AtMAP65-1 (WT) and the mutant, AtMAP65-1^{9D} (9D) phosphorylated with M-phase or S-phase (interphase, sampling point 0) extracts. The corresponding nitrocellulose membrane was stained with amido-black (Amidoblack).

kinases 2a and 2b), anti-MPK4 and 6 (mitogen-activated protein kinases 4 and 6) we pulled down CDKs and MAP kinases. All of these kinases phosphorylated AtMAP65-1 (Fig. 2C). Although the phosphorylation level of AtMAP65-1 was less when cdc2b and MPK4 were used, the reactions with control substrates had a similarly weaker signal indicating that the antibodies to cdc2b and MPK4 were less efficient in precipitating the kinase activity.

Identification of phorphorylation sites in AtMAP65-1

To determine the location of the phosphorylation site we generated four consecutive recombinant protein fragments covering the full-length AtMAP65-1 protein (Fragment 1, residues 1-150; Fragment 2, residues 151-339; Fragment 3, residues 340-494 and Fragment 4, residues 495-587). In phosphorylation assays using either the M-phase cell protein extract or the MAP preparation, only Fragment 4 was phosphorylated, indicating that all phosphorylation sites reside in this C-terminal region (Fig. 3A).

To further define the phosphorylation sites we generated nine synthetic peptides corresponding to AtMAP65-1 sequences in Fragment 4 that included kinase motifs. In phosphorylation assays using the M-phase cell extracts seven out of nine peptides were phosphorylated (Fig. 3B; Table 1). These peptides include motifs for cyclin-dependent kinases (S503, T526, S586), mitogen-activated protein kinase Erk1 (S543), aurora B cyclic nucleotide-dependent kinases (S532, T552) and casein kinase I and II protein kinase C (S539, T573, S576) indicating that all these kinases are potential regulators of AtMAP65-1. In total, there are nine phosphorylatable

Table 1. Prediction of phosphorylation sites in the synthetic peptides generated from sequences in AtMAP65-1 Fragment 4

Peptide	Sequence	Residue	Protein kinase	Reference	Mutants			
					2D	4D	7D	9D
1	QESAFSTRPSPA	S503	CDK,PKA,PKC	*, Scansite	+	+	+	+
3	ANGTHN	T526	CDK	Scansite			+	+
4	NRRLSLNA	S532	PKA,AuroraB, cAMK,cGMK	Scansite, Prosite		+	+	+
5	NGSRSTA	S540	CK1	Prosite				+
		T543	CK2,PKC	Prosite				+
6	RRETLNR	T552	cAMK,cGMK,PKA, PKC, AuroraB	Prosite,Scansite		+	+	+
8	AASSPVSGA	S573	CDK, Erk1	*, Disphos, PhosphoELM			+	+
		S576	CK1	†			+	+
9	QVPASP	S586	CDK	*, Disphos, PhosphoELM	+	+	+	+

+, corresponds to the amino acid residues substituted for aspartic acid in AtMAP65-1 phosphomimetics AtMAP65-1^{2D} (2D), AtMAP65-1^{4D} (4D), AtMAP65-1^{7D} (7D) and AtMAP65-1^{9D}(9D).

The phosphorylatable S/T residue is highlighted in bold within each peptide sequence.

CDK, cyclin-dependent protein kinase; PKA, protein kinase A; PKC, protein kinase C; cAMK, cAMP-dependent protein kinase; cGMK, cGMP-dependent protein kinase; CK1, casein kinase 1; CK2, casein kinase 2; Erk1, extracellular signal-regulated kinase 1.

*Kennelly and Krebs (Kennelly and Krebs, 1991); †Chang et al. (Chang et al., 2003).

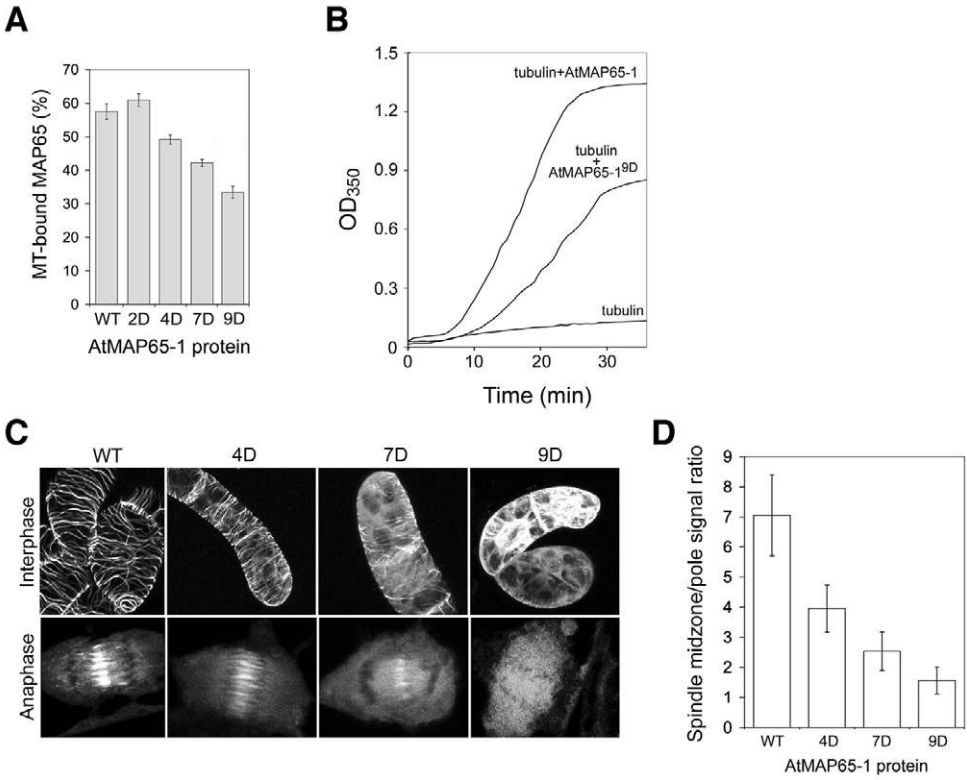

Fig. 4. Phosphorylation regulates the binding of AtMAP65-1 to microtubules. (A) Cosedimentation assays of taxol-stabilised microtubules with the recombinant wild-type AtMAP65-1 (WT) or the mutants, AtMAP65-1^{2D} (2D), AtMAP65-1^{4D}(4D), AtMAP65-1^{7D}(7D) and AtMAP65-1^{9D}(9D). The amount of AtMAP65-1 proteins in the supernatant and pellet was measured on the Coomassie-stained SDS-PAGE gels using densitometry and the percentage of the total recombinant AtMAP65-1 protein used in the reaction that was recovered in the pellet was calculated as described in the Materials and Methods. (B) Turbidimetric analysis of a 14 μM tubulin solution and a tubulin solution mixed in an equimolar ratio with AtMAP65-1 or AtMAP65-1^{9D}. (C) Localisation of GFP:AtMAP65-1^{4D}(4D), GFP:AtMAP65-1^{7D}(7D), GFP:AtMAP65-1^{9D}(9D) fusion proteins in interphase and anaphase cells. (D) The ratio between the midzone and the pole signals of GFP:AtMAP65-1 (WT), GFP:AtMAP65-1^{4D}(4D), GFP:AtMAP65-1^{7D}(7D) and GFP:AtMAP65-1^{9D}(9D) fusion proteins. Ten anaphase cells were analysed for each transgenic cell line.

residues, and we generated recombinant proteins where two, four, seven or nine of the residues were substituted for aspartic acid (AtMAP65-$1^{2D,4D,7D,9D}$; Table 1), a common phosphomimetic residue (Smertenko et al., 1998). We found that the level of AtMAP65-1^{9D} phosphorylation by M-phase extract was the same as the level by S-phase extract and similar to the level of wild-type protein phosphorylation by the S-phase extract (Fig. 3C). These data indicate that all kinase sites in AtMAP65-1 that are phosphorylated in mitosis have been abolished in this mutant.

AtMAP65-1 phosphomimetics have reduced binding to microtubules

Biochemical assays have been used to assess the microtubule-binding and bundling activity of the four phosphomimetic recombinant proteins (Table 1). The microtubule-binding assay was done using taxol stabilised pig brain microtubules. Microtubules (final concentration of tubulin 10 μM) and recombinant protein were mixed in a 1:1 molar ratio and centrifuged at 60,000 ***g*** for 10 minutes. The proteins in the pellet and supernatant were separated by SDS-PAGE and the amount of recombinant AtMAP65-1 in each sample was assessed by densitometry (Fig. 4A). The fraction of total phosphomimetic AtMAP65-1 protein used in the assay associated with microtubules decreased proportionally with the number of substituted residues. The maximum reduction in the MAP65 microtubule-binding activity was 40% when AtMAP65-1^{9D} was used. As a loading control the amount of tubulin in each pellet was measured and was found to be similar (data not shown). Next, we measured the effect of the AtMAP65-1 or AtMAP65-1^{9D} proteins on the turbidity of a tubulin solution. It has been shown that AtMAP65-1 has no prominent effect on the polymerisation dynamics of chromatographically purified pig brain tubulin (Wicker-Planquart et al., 2004; Smertenko et al., 2004), suggesting that increase in the turbidity of the tubulin solution upon addition of AtMAP65-1 protein results mainly from AtMAP65-1 bundling microtubules. As shown in the graph (Fig. 4B), the turbidity reading of tubulin mixed with AtMAP65-1^{9D} was 40% less than the turbidity value of tubulin mixed with AtMAP65-1, indicating that in this case reduced binding to microtubules results in a proportionally reduced MAP65 activity.

To determine whether in vitro data correlated with the behaviour of AtMAP65-1 phosphomimetics in vivo, we generated GFP chimeras with each of the mutants. Cell lines expressing these GFP chimeras were imaged and the data show that there is a progressive loss of microtubule-binding activity as the number of aspartate residues increases to nine (Fig. 4C). Previously we have shown using fluorescent recovery after photobleaching (FRAP) that GFP:AtMAP65-1 exhibits a dynamic interaction with microtubules and that this interaction is the same in the interphase cortical array, the preprophase band and the phragmoplast (Chang et al., 2005) indicating that this protein performs a similar function in these arrays. To determine whether the phosphomimetic proteins had altered microtubule interaction dynamics we performed FRAP on lines expressing GFP:AtMAP65-1^{9D}. The turnover of GFP:AtMAP65-1^{9D} was

Table 2. Analysis of the fluorescence recovery after photobleaching data of GFP:AtMAP65-1, GFP:AtMAP65-1^{9D}, GFP:AtMAP65-1^{9A} and tobacco homologue GFP:NtMAP65-1a

	k_{off}*	$t_{1/2}$ (s)	n	k_{off}†	Bound (%)
NtMAP65-1a					
Interphase‡	0.100	6.95±0.91	23	0.094	80.7
PPB‡	0.117	5.92±0.64	19	0.083	85.8
Metaphase‡	0.960	0.72±0.21	23	ND§	ND§
Phragmoplast‡	0.146	4.83±0.64	20	0.117	75.0
Oryzalin‡	0.402	1.71±0.24	23		
AtMAP65-1					
Interphase‡	0.117	5.93±0.86	20	0.081	67.4
AtMAP65-1^{9D}					
Phragmoplast	0.195	3.55±0.35	18	0.081	44.6
AtMAP65-1^{9A}					
Interphase	0.082	8.45±0.83	14	0.065	78.5
PPB	0.069	10.05±0.42	17	0.073	100.0
Metaphase	0.179	3.87±0.53	15	0.147	73.8
Phragmoplast	0.085	8.16±0.76	17	0.069	80.1

The dissociation constants k_{off} and $t_{1/2}$ were estimated for the GFP fusions in BY-2 cells at various cell cycle stages. n, the number of cells analysed in each experiment; Bound, the fraction of MAP65-1:GFP initially bound to the microtubules, expressed as percentages of total fusion protein. *k_{off} estimated by single exponential fit; †k_{off} estimated by double exponential fit; ‡Chang et al. (Chang et al., 2005); §Not determined because values were below the threshold for diffusion seen in the oryzalin-treated control cells.

compared with the turnover of NtMAP65-1a, which has similar microtubule-binding dynamics to GFP:AtMAP65-1 (Chang et al., 2005). The turnover of AtMAP65-1^{9D} was found to be faster and the amount bound to microtubules reduced by 40%, which corresponds directly with the same reduction in microtubule-binding activity in vitro (Table 2). Furthermore, there is a concomitant reduction in MAP65 binding to the anaphase spindle midzone. The ratio between GFP signal in the anaphase spindle midzone and the spindle poles was four times less than in the line expressing GFP:AtMAP65-1^{9D} compared with the control (Fig. 4D). The ability of AtMAP65-1 phosphomimetics to concentrate at the anaphase spindle midzone was affected more than their ability to bind microtubules, strongly suggesting that dephosphorylation of MAP65 is necessary not only for microtubule binding or bundling but also for the correct localisation of this protein in vivo during anaphase-telophase. Reduced accumulation at the spindle midzone of AtMAP65-1 phosphomimetics resembles the effect of okadaic acid on wild-type GFP:AtMAP65-1-expressing cell lines (compare Fig. 2G with Fig. 5C) supporting a conclusion that the level of phosphorylation is important for controlling MAP65 activity.

Binding of AtMAP65-1 to microtubules during prophase and metaphase affects mitosis

As the AtMAP65-1 phosphomimetic protein gives the same phenotype in vivo as the treatment with phosphatase inhibitors

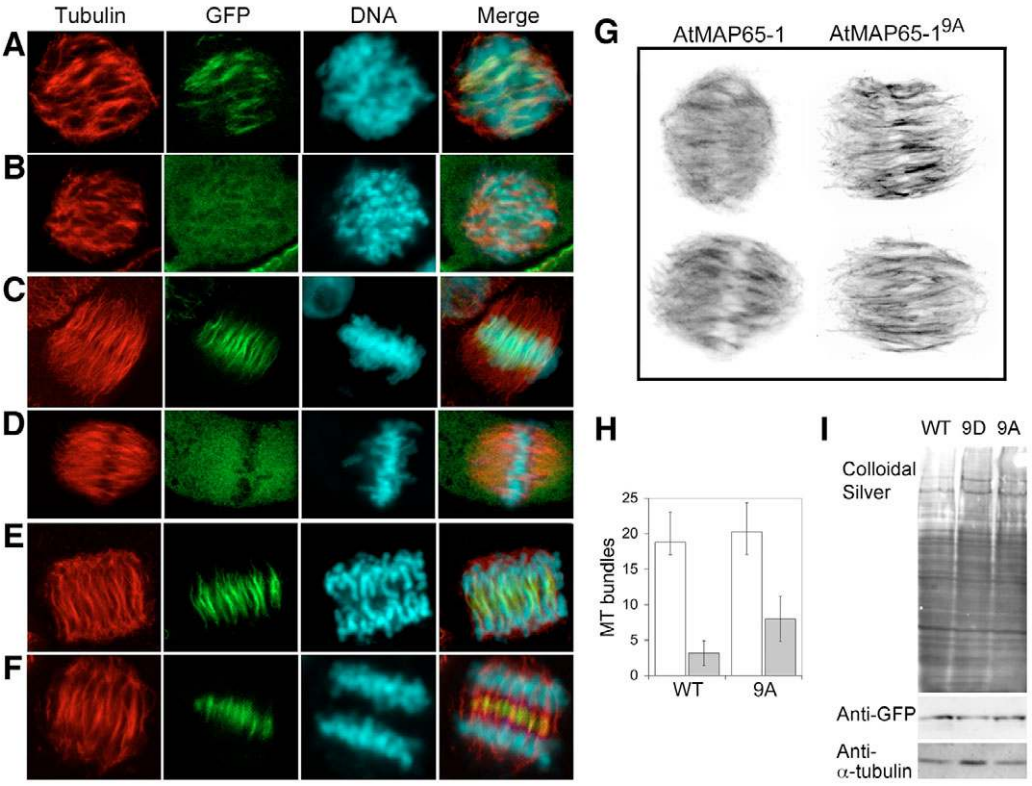

Fig. 5. Non-phosphorylatable AtMAP65-1 binds spindle microtubules and affects metaphase spindle organisation. (A-F) Immunolocalisation of tubulin (red), GFP:AtMAP65-1 (green, B,D,F) and GFP:AtMAP65-1^{9A} (green, A,C,E), DNA (blue) during prometaphase (A,B), metaphase (C,D) and anaphase (E,F). The wild-type protein becomes associated with microtubules only in anaphase whereas the alanine mutant binds to microtubules in prophase and metaphase. (G) Negative images of the typical microtubule pattern in metaphase spindles of cell lines expressing GFP:AtMAP65-1 or GFP:AtMAP65-1^{9A}. The cells are immunostained with an antibody to α-tubulin, DM1A. Note the microtubules are excessively bundled in the GFP:AtMAP65-1^{9A} spindles. (H) Number of all microtubules (white bars) and the number of pole to pole microtubules (grey bars) visible in a 1 μm optical section in the spindles of cells expressing GFP:AtMAP65-1 (WT) or GFP:AtMAP65-1^{9A} (9A). Twenty cells were analysed for WT and 18 for 9A (P<0.05) from two different cell lineages. (I) Western blot of total cell protein extracts from the BY-2 cell lines expressing wild-type GFP:AtMAP65-1 (WT), GFP:AtMAP65-1^{9D} (9D) or GFP:AtMAP65-1^{9A} (9A) probed with anti-GFP and anti-α-tubulin antibody. The colloidal silver stain shows the general pattern of proteins transferred onto the nitrocellulose membrane.

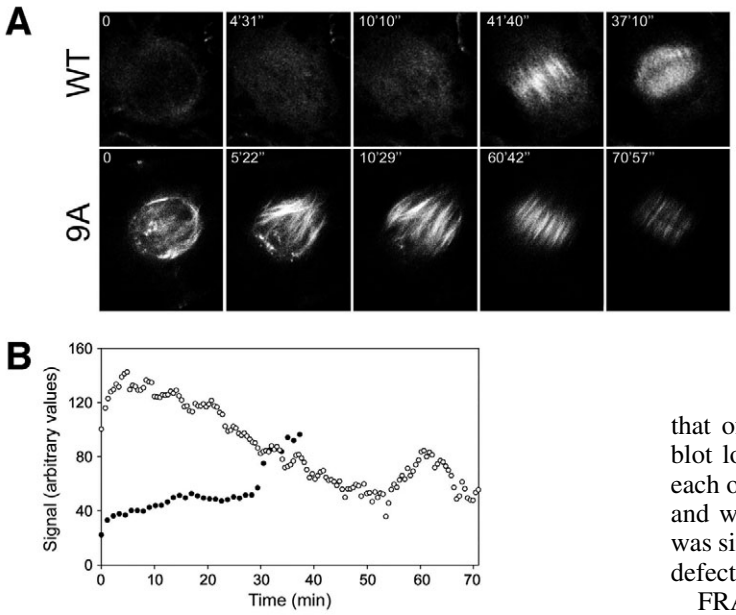

Fig. 6. Expression of non-phosphorylatable AtMAP65-1 delays the metaphase/anaphase transition. (A) Localisation of wild-type GFP:AtMAP65-1 (WT) and mutant GFP:AtMAP65-1^{9A} (9A) fusions during mitosis. The wild-type protein becomes associated with microtubules only in anaphase whereas the mutant binds to microtubules at every stage of mitosis. Numbers in the top right corner indicate timing of each frame. (B) Quantification of the fluorescent signal in the cell division midzone of GFP:AtMAP65-1 (closed circles) and GFP:AtMAP65-1^{9A} (open circles).

then the converse ought to be true. That is, if all these sites were to be made non-phosphorylatable (by replacing the nine phosphorylatable residues with alanine) and the experiments in vivo repeated we should get similar results to the GFP:AtMAP65-1 lines treated with kinase inhibitors. We therefore generated AtMAP65-1 mutants where all nine sites were replaced with alanine. Cell lines expressing GFP:AtMAP65-1^{9A} were made. Double immunostaining with anti-tubulin and live cell imaging revealed that microtubules in prophase and metaphase were bound by this protein thereby phenocopying the cell lines treated with the kinase inhibitors (Fig. 5A-F, compare with Fig. 2D,E). During anaphase/telophase the localisation of GFP:AtMAP65-1^{9A} and wild-type protein were similar, except that the GFP signal occupied a wider zone in the middle of the spindle and was decorating notably thicker microtubule bundles (Fig. 5E,F). AtMAP65-1^{9A} binding to metaphase spindle microtubules resulted in abnormal spindle morphology. Fig. 5G shows negative images of anti-tubulin staining in several typical spindles of the cell lines expressing GFP:AtMAP65-1 and GFP:AtMAP65-1^{9A}. An increase in the number of microtubules apparently crossing the midzone (pole-to-pole microtubules) of the mitotic spindle was observed in the cells expressing GFP:AtMAP65-1^{9A}. We have compared the number of pole-to-kinetochore microtubules and the number of pole-to-pole microtubules in a 1 μm thick optical section through the centre of the spindle taken using confocal laser microscopy. Microtubules terminating at the area of the spindle occupied by the chromosomes were considered as pole-to-kinetochore, whereas microtubules crossing this region were considered as pole-to-pole. The total number of microtubules found in each optical section was similar in both lines, however, the number of pole-to-pole microtubules was 2.5 times higher in the cell line expressing AtMAP65-1^{9A} (Fig. 5H). Therefore, binding of AtMAP65-1 to microtubules during metaphase spindle formation affects the spatial arrangement of microtubules.

The expression level of AtMAP65-1^{9A} was compared with that of AtMAP65-1 and AtMAP65-1^{9D} (Fig. 5I). A western blot loaded with equal amounts of total protein extract from each of the three cell lines was probed with anti-GFP antibody and with anti-α-tubulin as a control. The level of expression was similar for each of the chimeric proteins indicating that the defects seen were solely due to the activity of AtMAP65-1^{9A}.

FRAP analysis showed a dramatic change in the dynamics of the interaction of AtMAP65-1^{9A} with microtubules in vivo, especially during spindle formation. The rate of GFP:AtMAP65-1^{9A} turnover on microtubules is two-fold slower in the cortical microtubule array, PPB and phragmoplast, and five times slower in the metaphase spindle compared to the wild-type protein. Calculation of the proportion of GFP:AtMAP65-1^{9A} associated with microtubules in the mitotic spindle shows that 73.8% of the protein is associated with microtubules whereas the wild-type protein is not bound to microtubules (Table 2). These data indicate that the association of AtMAP65-1^{9A} with microtubules during prophase/metaphase is the result of reduced protein turnover.

We determined whether aberrant spindle morphology affects the normal metaphase/anaphase transition. To do this the intensity of the fluorescence signal was measured in a 5 μm diameter circle positioned at the centre of the future cell plate. The GFP signal was analysed starting from the first time frame when the PPB disassembled (Fig. 6A row WT time point 0) and until the appearance of the clear zone in the middle of phragmoplast (Fig. 6A row WT time point 37′10′′); a microtubule-free zone in the equatorial part of the phragmoplast occupied by the newly formed cell plate (Segui-Simarro et al., 2004). Three different cell lines were analysed in this experiment and two cells were imaged per line, producing similar data. A typical example is shown in Fig. 6B. In cells expressing the GFP:AtMAP65-1, the fluorescence signal was weak until the onset of anaphase, whereas in the cell expressing AtMAP65-1^{9A} the signal stayed high and then gradually decreased and increased again before the appearance of the clear zone in the phragmoplast (Fig. 6B row 9A, time point 70′57′′). The time taken for the cell to form a mitotic spindle and go through anaphase and cell plate initiation was almost twofold longer in the cell lines expressing AtMAP65-1^{9A}. The relative abundance of pole-to-pole microtubules must therefore interfere with normal spindle function.

Discussion

We have identified a region in AtMAP65-1 that is phosphorylated by kinase extracts, and mapped nine potential

phosphorylation sites within this region. Mutation of these sites to alanine to generate non-phosphorylatable AtMAP651^{9A} and expression of this protein in suspension culture cells revealed that AtMAP651^{9A} bound microtubules in metaphase. Replacement of the same amino acids with aspartic acid, AtMAP651^{9D}, diminished microtubule binding throughout the cell cycle. The consequence of AtMAP651^{9A} binding microtubules was to delay mitotic progression.

The major activity of MAP65 proteins is microtubule bundling and the formation of 25 nm cross-bridges between microtubules. In both interphase and mitotic microtubule arrays MAP65 is thought to cross-link and bundle microtubules. The *S. pombe* MAP65 homologue Ase1p localises to sites of overlap of antiparallel microtubules and the mutant, *ase1*, loses anti-parallel microtubule structures (Loïodice et al., 2005). MAP65 also localises to regions of overlapping antiparallel microtubules in the mitotic arrays. Strikingly, all MAP65s that accumulate in the anaphase spindle midzone exhibit no interaction with metaphase spindle microtubules (Van Damme et al., 2004; Smertenko et al., 2004), suggesting that their interaction with microtubules must be under tight cell cycle control. When a non-phosphorylatable form of AtMAP65-1, AtMAP65-1^{9A}, was expressed in suspension culture cells, excessive microtubule bundling was observed and this resulted in the delay of the onset of anaphase. The turnover of non-phosphorylatable GFP: AtMAP65-1^{9A} in the metaphase spindle was similar to the turnover of wild-type GFP:AtMAP65-1 in the phragmoplast, indicating that mobility of AtMAP65-1^{9A} within bundles was not unusual. Excessive microtubule bundling caused a delay in the metaphase/anaphase transition possibly because of the obstruction of chromosome positioning by the rigidity imposed by excessive bundling.

If phosphorylation of AtMAP65-1 abolishes its binding to microtubules during metaphase, then anaphase onset must be accompanied by a phosphatase activity that will dephosphorylate AtMAP65-1, restoring its ability to bind microtubules. It is probable that a phosphatase of type 1 or 2A dephosphorylates AtMAP65-1 because okadaic acid, a phosphatase type 1 and 2A inhibitor, reduced the binding of AtMAP65-1 to phragmoplast microtubules. However, even if a phosphatase restores microtubule binding the protein still must localise to the midzone. Human PRC1 interacts with a plus end directed kinesin, KIF4, and it has been shown that depleting KIF4 results in PRC1 not accumulating at the midzone, indicating that a kinesin is involved in this movement (Kurasawa et al., 2004; Zhu and Jiang, 2005). A similar mechanism was suggested to explain the accumulation of *Schizosaccharomyces pombe* Ase1p at microtubule nucleating centres but using a minus end directed kinesin (Loïodice et al., 2005). Interestingly, phosphorylation of PRC1 inhibits its interaction with KIF4 indicating that accumulation at the midzone coordinated by KIF4 is regulated by phosphorylation (Zhu and Jiang, 2005). The phosphomimetic AtMAP65-1^{9D} had a reduced microtubule-binding activity (by 40%), but was virtually absent from the division midzone suggesting that phosphorylation also controls accumulation in the midzone. AtMAP65-1^{9A}, which could not be phosphorylated, bound microtubules in the mitotic spindle and localised preferentially to the spindle midzone. Our data indicate that phosphorylation controls both binding of AtMAP65-1 to microtubules and its targeting to the midzone. Several *Arabidopsis* kinesins have been shown to localise to the spindle midzone (e.g. Lee and Liu, 2000; Strompen et al., 2002) and it remains to be determined if one of these can target AtMAP65-1 to the spindle midzone. Indeed a KIF4 homologue is listed in the Arabidopsis Genome database (Mao et al., 2005).

Although the excessive bundling of microtubules by MAP65-like proteins has an inhibitory effect on mitosis in plants, animals and yeasts (Juang et al., 1997; Mollinari et al., 2002), different mechanisms have been employed for the control of this activity. *S. cerevisiae* Ase1p, for example, is controlled by cell cycle-specific degradation (Juang et al., 1997) using the anaphase promoting complex (APC) pathway. Human PRC1 was first identified as a CDK substrate (Jiang et al., 1998), and knocking out the two CDK sites caused an increase in microtubule bundling during metaphase and this excessive bundling blocked the metaphase to anaphase transition. However, the PRC1 phosphomimetic bound microtubules (Mollinari et al., 2002). In plants it is probable that the activity of MAP65-like proteins during mitosis is regulated in a stage-specific manner by multiple kinase pathways. Although our data indicate that simultaneous activity of several protein kinases, including CDK and MAPK, is required for control of MAP65-1 in metaphase, in telophase the control is reliant on the MAP kinase pathway and not the CDK pathway (Sasabe et al., 2006). The level of AtMAP65-1 phosphorylation increases in G2, peaks in prometaphase, stays high in metaphase and then gradually decreases towards G1. Alanine substitution of one of the CDK sites (S503) (Mao et al., 2005) in AtMAP65-1 was sufficient to restore its binding to microtubules during metaphase, but had no effect on mitosis. Moreover, as we show here, increased activity of the CDK pathway in the cell line expressing non-degradable cyclin B is not sufficient to inhibit the association of MAP65 with microtubules in the phragmoplast. These data would suggest that hyperphosphorylation of AtMAP65-1 by multiple kinases is essential to inhibit the binding of AtMAP65-1 to microtubules in mitosis.

Both CDK and MAPK are known microtubule-interacting proteins (Fellous et al., 1994; Reszka et al., 1995) and we have shown that the microtubule protein preparation phosphorylated AtMAP65-1, implying that while bound to microtubules MAP-65 could be phosphorylated by the microtubule-associated kinases. The effect of this phosphorylation would be to decrease the affinity of AtMA65-1 for microtubules and locally change microtubule bundling. CDKs and MAPKs colocalise with microtubules in M-phase and were also found in the midzone of anaphase spindle and the phragmoplast (Bögre et al., 1999; Weingartner et al., 2001). However, CDK has been shown not to be involved in the control of NtMAP65-1a in the phragmoplast (Sasabe et al., 2006). Disruption of the MAP kinase pathway causes abnormal cytokinesis resulting from the inhibition of phragmoplast expansion (Nishihama et al., 2001) and mutation of the MAPK phosphorylation site in NtMAP65-1a delays cytokinesis.

Previously we reported that AtMAP65-1 binds to only polymerised microtubules, indicating that two tubulin molecules from the same or adjacent protofilaments are involved in this interaction (Chang et al., 2005). Two microtubule interaction sites are essential for MAP65 activity (Smertenko et al., 2004). One site is located between amino

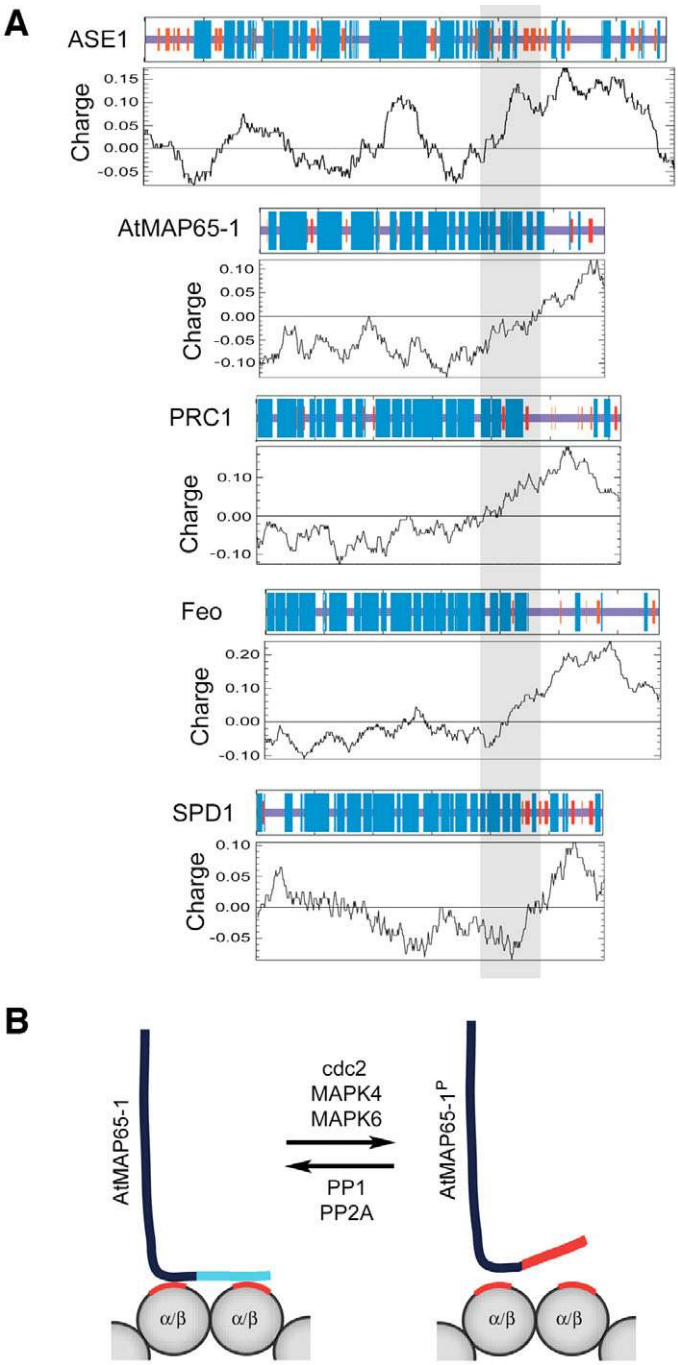

Fig. 7. A model for the mechanism of AtMAP65-1 regulation. (A) Diagrams of the secondary structure prediction and charts of charge distribution for anaphase spindle elongation protein 1 (ASE1), AtMAP65-1, PRC1, Feo and spindle defective 1 (SPD1). Blue colour represents α helices, red represents β strand and violet represents coiled coil. (B) Scheme for the interaction between AtMAP65-1 and microtubules. Two microtubule-interacting sites on AtMAP65-1 are needed for normal function. One site is not affected by phosphorylation and is not coloured, the second site is normally alkaline (shown is blue). The alkaline region binds to the acidic C-terminal region of tubulin (shown in red). After phosphorylation the charge of the second microtubule-interacting site changes to acidic (shown in red). This weakens the binding of AtMAP65-1 to microtubules.

acids 339 and 494 and it is conserved within all members of the MAP65/Ase1p family (shaded in Fig. 7A). Downstream of this site there is another microtubule interaction site, the extreme C-terminal coiled coil basic region. This region exhibits no primary structure conservation across the *Arabidopsis* MAP65 family, but is preferentially coiled coil and basic within this family and in the other members of the MAP-65/Ase1p family (Fig. 7A). It has been shown that cleavage of a 2 kDa C-terminal fragment from tubulin using the protease subtilisin, inhibits the binding of MAP-65 to microtubules (Wicker-Planquart et al., 2004). This region of tubulin is acidic, exposed on the microtubule surface and is a known interface for interaction with microtubule-associated proteins (Ludueña et al., 1992) suggesting that association between microtubules and the second microtubule interaction site of MAP-65 is based on a charge interaction. Correspondingly, all known phosphorylation sites of AtMAP65-1 as well as PRC1 (Jiang et al., 1998) and NtMAP65-1a (Sasabe et al., 2006) are located within the second microtubule interacting region. Phosphorylation of these sites raises the pI of this region from alkaline (10.6) to acidic (max 5.3) but does not significantly effect the pI of the whole molecule (from 5.7 to 5.5). Consequently, the interaction between this region in its phosphorylated form and a microtubule diminishes (Fig. 7B). The activity of type 1 and 2A protein phosphatases in such a model is then required to restore AtMAP65-1 binding to microtubules.

Materials and Methods

Tissue culture, synchronisation and treatments

Nicotiana tabacum Bright Yellow-2 (BY-2) suspension cells were cultured in MS medium containing 30 g/l sucrose, 370 mg/ml KH_2PO_4, 1.0 mg/ml thiamine hydrochloride and 0.2 mg/ml 2,4-dichlorophenoxyacetic acid and synchronised as described previously (Kakimoto and Shibaoka, 1988). The cells were grown at 26°C with orbital shaking at 160 rotations per minute; for the subculturing, 2 ml of a 1-week-old culture were inoculated into 100 ml of the medium. Protein kinase inhibitors DMAP (5 mM), olomoucine (100 μM) or protein phosphatase inhibitor okadaic acid (10 μM) were added to a 3-day-old BY-2 cell line expressing GFP:AtMAP65-1 (Chang et al., 2005). Cells were mounted under coverslips and imaged immediately using a Zeiss 510 inverted confocal laser microscope. The first effects of the inhibitors were detected after 5 minutes and these became more prominent after 10 minutes.

Recombinant protein expression and purification

Full-length recombinant AtMAP65-1, mutants thereof and fragments 1-4 were expressed and purified as reported earlier (Smertenko et al., 2004). Putative phosphorylatable residues were mutated using the QuickChangeMulti site-directed mutagenesis kit (Stratagene, UK) according to manufacturer's recommendations.

GFP imaging, immunostaining and image analysis

Construction of the GFP fusions with wild-type AtMAP65-1 and mutant AtMAP65-1, and plant transformation were done as described previously (Chang et al., 2005). GFP imaging and fluorescence recovery after photobleaching (FRAP) experiments were also done as described previously (Chang et al., 2005). For the analysis of GFP signal dynamics in the division midzone during prophase/metaphase/anaphase, the fluorescence intensity was measured in a circle of 5 μm in diameter positioned approximately in the centre of the nucleus where the future cell plate will be positioned. The time between the disappearance of the pre-prophase band and formation of the GFP:AtMAP65-1-free zone in the phragmoplast (Chang et al., 2005) was calculated in six cells. The background value was recorded outside the division midzone and then subtracted from the original values. Two representative examples are shown in the Fig. 4E.

Tubulin immunostaining in BY-2 cells expressing GFP:AtMAP65-1 and GFP:AtMAP65-1^{9A} was done as described (Smertenko et al., 2004). Mouse monoclonal anti-tubulin antibody clone DM1A (Sigma) was diluted 1:100. Anti-mouse TRITC-conjugated secondary antibody (Jackson ImmunoResearch) was diluted 1:200.

Microtubules in mitotic spindles of transfected cell lines harbouring wild-type and mutant AtMAP65-1 were compared using images from single optical sections recorded in cells from two independent cell lineages. Microtubules crossing the

chromosome plane were counted as pole-to-pole microtubules and the fibres terminating at the chromosome plane were counted as pole-to-kinetochore microtubules.

Protein extraction, immunoprecipitation and phosphorylation assays

Protein was extracted from BY-2 cells and phosphorylation assays were setup as described previously (Bögre et al., 1997). Each phosphorylation reaction contained 5 μg of either recombinant AtMAP65-1, one of its fragments, or mutated AtMAP65-1 and 1 μg of total protein extract where appropriate. The reaction was allowed to proceed for 20 minutes then samples were mixed with 4× SDS-PAGE sample buffer, boiled for 3 minutes and run on 10% or 15% SDS-PAGE gels. The gels were stained with Coomassie Brilliant Blue R250 and dried or transferred onto nitrocellulose membrane and exposed to X-ray film. In the protein kinase inhibitor experiments 2 mM DMAP, 5 μM K525a, 5 μM staurosporine or 100 μM olomoucine were added to the kinase and incubated for 5 minutes before the substrate was added.

Kinases were precipitated using Suc1 beads, anti-cdc2a, anti-cdc2b, anti-MPK4 and anti-MPK6 as described by Bögre et al. (Bögre et al., 1997). Histone 1 (5 μg) was used as a positive control for the phosphorylation reactions with cyclin-dependent kinases, and myelin basic protein (MBP; 5 μg) was used as a positive control for phosphorylation reactions with mitogen-activated protein kinases. The reaction was performed according to Bögre et al. (Bögre et al., 1997).

Electrophoresis and western blotting

Protein samples for two dimensional SDS-PAGE were prepared as described previously (Hussey and Gull, 1985). Samples were analysed using 18-cm, linear, immobilised pH 4-7 gradient IPG (immobilised pH gradient) strips (Amersham). 50-70 μg of protein were resuspended in rehydration buffer containing 7 M urea, 2 M thiourea, 4% CHAPS, 30 mM DTT, 0.2% vol/vol ampholines pH 4-7 (Amersham, UK) and a trace amount of Bromophenol Blue. The strips were rehydrated overnight at room temperature under mineral oil. Isoelectric focusing was carried out using a Multiphor II flatbed apparatus (Amersham Biosciences) at 16°C: the voltage was first linearly increased from 0 to 500 V for 1 minute, then linearly increased to 3500 V for 1 hour 30 minutes and finally kept at 3500 V for 7 hours 40 minutes. Current and power settings were limited to 40 mA and 5 W per strip. For the second-dimension SDS-PAGE, IPG strips were agitated at room temperature for 10 minutes in equilibration buffer [50 mM Tris-HCl, pH 8.8, 6 M urea, 30% (v/v) glycerol, 2% (w/v) SDS] supplemented with 2% (w/v) DTT and for 10 minutes in the equilibration buffer supplemented with 2.5% (w/v) iodoacetamide. Strips were mounted on top of 7.5% or 10% SDS-PAGE gels and overlaid with 1% (w/v) agarose solution in SDS-PAGE running buffer containing a trace amount of Bromophenol Blue. Electrophoresis was carried using an Ettan Dalt*six* Electrophoresis System (Amersham) at 100 V/gel at 16°C. Gels were stained with Coomassie Blue R-250 (BDH, England). The western blotting was done according to Smertenko et al. (Smertenko et al., 2004). Anti-AtMAP65-1 (Smertenko et al., 2004), α-tubulin (clone DM1A, Sigma, Dorset, UK) and GFP (Abcam, UK) antibodies were diluted 1:1000.

Microtubule cosedimentation and turbidimetric assays

Cosedimenation assays of all the AtMAP65-1 recombinant proteins with microtubules were done as described in Smertenko et al. (Smertenko et al., 2004) with the following modification. Taxol stabilised microtubules and recombinant AtMAP65-1 proteins were mixed to a final concentration of 10 μM and centrifuged for 10 minutes at 60,000 ***g***. The samples of supernatant and pellet after centrifugation were adjusted to 100 μl, mixed with an equal amount of 2× SDS-PAGE sample buffer and heated at 95°C for 5 minutes. A 20 μl aliquot of each sample was run on a 10% SDS-PAGE gels. The gels were stained with Coomassie Brilliant Blue R-250 and scanned using a flat bed scanner. The amount of protein on the gel was quantified using NIH image software version 1.62 (National Institute of Health, USA). For the quantification of each protein band, local values for the background were estimated and subtracted from each protein band value. Then the data from each of the three replicates were normalised using the mean: the intensity for each band in a particular replicate was divided by the mean intensity for all bands in the replicate. The normalised values were used to calculate the percentage of the AtMAP65-1 protein in the pellet. Almost all the tubulin was in the pellet after the addition of Taxol and the amount of tubulin in the pellet for each sample was used as a loading control.

For the turbidimetric analysis, 15 μM tubulin solution on its own or mixed with recombinant AtMAP65-1 in an equimolar ratio was measured at 350 nm for 35 minutes as described by Smertenko et al. (Smertenko et al., 2004).

Bioinformatics

Protein kinase motifs were predicted using programmes Prosite (http://www.expasy.org/prosite/), Scansite (http://scansite.mit.edu/), Disphos (http://core.ist.temple.edu/pred/) and PhosphoELM (http://phospho.elm.eu.org/pictures/phospho.logo.png). The secondary structure was predicted using program HNN at http://pbil.ibcp.fr/htm/ (Combet et al., 2000). Protein charge plots were generated using Charge program of EMBOSS package at http://bioweb.pasteur.fr/seqanal/protein/ using 100 amino acid window size.

This work was funded in part by the Biotechnology and Biological Sciences Research Council and by Overseas Research Students award to H.-Y. Chang. We would like to thank Chris Jones for technical help.

References

Bögre, L., Zwerger, K., Meskiene, I., Binarova, P., Csizmadia, V., Planck, C., Wagner, E., Hirt, H. and Heberle-Bors, E. (1997). The cdc2Ms kinase is differently regulated in the cytoplasm and in the nucleus. *Plant Physiol.* **113**, 841-852.

Bögre, L., Calderini, O., Binarova, P., Mattauch, M., Till, S., Kiegerl, S., Jonak, C., Pollaschek, C., Barker, P., Huskisson, N. S. et al. (1999). A MAP kinase is activated late in plant mitosis and becomes localized to the plane of cell division. *Plant Cell* **11**, 101-113.

Chan, J., Jensen, C. G., Jensen, L. C. W., Bush, M. and Lloyd, C. W. (1999). The 65-kDa carrot microtubule-associated protein forms regularly arranged filamentous cross-bridges between microtubules. *Proc. Natl. Acad. Sci. USA* **96**, 14931-14936.

Chang, E. J., Archambault, V., McLachlin, D. T., Krutchinsky, A. N. and Chait, B. T. (2003). Analysis of protein phosphorylation by hypothesis-driven multiple-stage mass spectrometry. *Anal. Chem.* **76**, 4472-4483.

Chang, H.-Y., Smertenko, A. P., Igarashi, H., Dixon, D. P. and Hussey, P. J. (2005). Dynamic interaction of NtMAP65-1a with microtubules in vivo. *J. Cell Sci.* **118**, 3195-3201.

Combet, C., Blanchet, C., Geourjon, C. and Deléage, G. (2000). NPS@: network protein sequence analysis. *Trends Biochem. Sci.* **25**, 147-150.

Fellous, A., Kubelka, M., Thibier, C., Taieb, F., Haccard, O. and Jessus, C. (1994). Association of p34(cdc2) kinase and map kinase with microtubules during the meiotic maturation of xenopus oocytes. *Int. J. Dev. Biol.* **38**, 651-659.

Glotzer, M. (2005). The molecular requirements for cytokinesis. *Science* **307**, 1735-1739.

Hush, J. M, Wadsworth, P., Callaham, D. A. and Hepler, P. K. (1994). Quantification of microtubule dynamics in living plant cells using fluorescence redistribution after photobleaching. *J. Cell Sci.* **107**, 775-784.

Hussey, P. J. and Gull, K. (1985). Multiple isotypes of alpha-tubulin and beta-tubulin in the plant phaseolus-vulgaris. *FEBS Lett.* **181**, 113-118.

Hussey, P. J., Hawkins, T. J., Igarashi, H., Kaloriti, D. and Smertenko, A. (2002). The plant cytoskeleton: recent advances in the study of the plant microtubule-associated proteins MAP-65, MAP-190 and the *Xenopus* MAP215-like protein, MOR1. *Plant Mol. Biol.* **50**, 915-924.

Jiang, C. J. and Sonobe, S. (1993). Identification and preliminary characterization of a 65kDa higher-plant microtubule-associated protein. *J. Cell Sci.* **105**, 891-901.

Jiang, W., Jimenez, G., Wells, N. J., Hope, T. J., Wahl, G. M., Hunter, T. and Fukunaga, F. (1998). PRC1: a human mitotic spindle-associated CDK substrate protein required for cytokinesis. *Mol. Cell* **2**, 877-885.

Juang, Y.-L., Huang, J., Peters, J.-M., McLaughlin, M. E., Tai, C.-Y. and Pellman, D. (1997). APC-mediated proteolysis of Ase1 and the morphogenesis of the mitotic spindle. *Science* **275**, 1311-1314.

Kakimoto, T. and Shibaoka, H. (1988). Cytoskeletal ultrastructure of phragmoplast-nuclei complexes isolated from cultured tobacco cells. *Protoplasma* (Suppl.) **2**, 95-103.

Kennelly, P. J. and Krebs, E. G. (1991). Consensus sequences as substrate-specificity determinants for protein-kinases and protein phosphatases. *J. Biol. Chem.* **266**, 15555-15558.

Kline-Smith, S. L. and Walczak, C. E. (2004). Review mitotic spindle assembly and chromosome segregation: refocusing on microtubule dynamics. *Mol. Cell* **15**, 317-327.

Kurasawa, Y., Earnshaw, W. C., Mochizuki, Y., Dohmae, N. and Todokoro, N. (2004). Essential roles of KIF4 and its binding partner PRC1 in organized central spindle midzone formation. *EMBO J.* **23**, 3237-3248.

Lee, Y.-R. J. and Liu, B. (2000). Identification of a phragmoplast-associated kinesin-related protein in higher plants. *Curr. Biol.* **10**, 797-800.

Loïodice, I., Staub, J., Setty, T. J., Nguyen, N.-P. T., Paoletti, A. and Tran, P. T. (2005). Ase1p organizes antiparallel microtubule arrays during interphase and mitosis in fission yeast. *Mol. Biol. Cell* **16**, 1756-1768.

Ludueña, R. F., Banerjee, A. and Khan, I. A. (1992). Tubulin structure and biochemistry. *Curr. Opin. Cell Biol.* **4**, 53-57.

Mao, G., Chan, J., Calder, G., Doonan, J. H. and Lloyd, C. W. (2005). Modulated targeting of GFP-AtMAP65-1 to central microtubules during division. *Plant J.* **43**, 469-478.

Mollinari, C., Kleman, J. P., Jiang, W., Schoehn, G., Hunter, T. and Margolis, R. L. (2002). PRC1 is a microtubule binding and bundling protein essential to maintain the mitotic spindle midzone. *J. Cell Biol.* **157**, 1175-1186.

Müller, S., Smertenko, A., Wagner, V., Heinrich, M., Hussey, P. J. and Hauser, M.-T. (2004). The plant microtubule associated protein, AtMAP65-3/PLE, is essential for cytokinetic phragmoplast function. *Curr. Biol.* **14**, 412-417.

Nishihama, R. and Machida, Y. (2001). Expansion of the phragmoplast during plant cytokinesis: a MAPK pathway may MAP it out. *Curr. Opin. Plant Biol.* **4**, 507-512.

Nishihama, R., Ishikawa, M., Araki, S., Soyano, T., Asada, T. and Machida, Y. (2001). The NPK1 mitogen-activated protein kinase kinase is a regulator of cell-plate formation in plant cytokinesis. *Genes Dev.* **15**, 352-363.

Otegui, M. S., Verbrugghe, K. J. and Skop, A. R. (2005). Midbodies and phragmoplasts: analogoues structures involved in cytokinesis. *Trends Cell Biol.* **15**, 404-413.

Pellman, D., Bagget, M., Tu, H. and Fink, G. R. (1995). Two microtubule-associated proteins required for anaphase spindle movement in Saccharomyces cerevisiae. *J. Cell Biol*. **130**, 1375-1385.

Reszka, A. A., Seger, R., Diltz, C. D., Krebs, E. G. and Fischer, E. H. (1995). Association of mitogen-activated protein-kinase with the microtubule cytoskeleton. *Proc. Natl. Acad. Sci. USA* **92**, 8881-8885.

Sasabe, M., Soyano, S., Takahashi, Y., Sonobe, S., Igarashi, H., Itoh, T. J., Hidaka, M. and Machida, Y. (2006). Phosphorylation of NtMAP65-1 by a MAP kinase down-regulates its activity of microtubule bundling and stimulates progression of cytokinesis of tobacco cells. *Genes Dev.* **20**, 1004-1014.

Saxton, W. M., Stemple, D. L., Leslie, R. J., Salmon, E. D., Zavortink, M. and McIntosh, J. R. (1984). Tubulin dynamics in cultured mammalian cells. *J. Cell Biol*. **99**, 2175-2186.

Segui-Simarro, J. M., Austin, J. R., II, White, E. A. and Staehelin, L. A. (2004). Electron tomographic analysis of somatic cell plate formation in meristematic cells of Arabidopsis preserved by high-pressure freezing. *Plant Cell* **16**, 836-856.

Smertenko, A., Saleh, N., Igarashi, H., Mori, H., Hauser-Hahn, I., Jiang, C. J., Sonobe, S., Lloyd, C. W. and Hussey, P. J. (2000). A new class of microtubule-associated proteins in plants. *Nat. Cell Biol.* **2**, 750-753.

Smertenko, A. P., Jiang, C.-J., Simmons, N. J., Weeds, A. G., Davies, D. R. and Hussey, P. J. (1998). Ser6 in the maize actin-depolymerizing factor, ZmADF3, is phosphorylated by a calcium-stimulated protein kinase and is essential for the control of functional activity. *Plant J.* **14**, 187-194.

Smertenko, A. P., Chang, H. Y., Wagner, V., Kaloriti, D., Fenyk, S., Sonobe, S., Lloyd, C., Hauser, M. T. and Hussey, P. J. (2004). The *Arabidopsis* microtubule-associated protein AtMAP65-1: molecular analysis of its microtubule bundling activity. *Plant Cell* **16**, 2035-2047.

Strompen, G., El Kasmi, F., Richter, S., Lukowitz, W., Assaad, F. F., Jurgens, G. and Mayer, U. (2002). The *Arabidopsis HINKEL* gene encodes a kinesin-related protein involved in cytokinesis and is expressed in a cell cycle-dependent manner. *Curr. Biol.* **22**, 153-158.

Van Damme, D., Van Poucke, K., Boutant, E., Ritzenthaler, C., Inze, D. and Geelen, D. (2004). In vivo dynamics and differential microtubule-binding activities of MAP65 proteins. *Plant Physiol*. **136**, 3956-3967.

Verbrugghe, K. J. C. and White, J. G. (2004). SPD-1 is required for the formation of the spindle midzone but is not essential for the completion of cytokinesis in C. elegans embryos. *Curr. Biol*. **14**, 1755-1760.

Verde, F., Labbe, J. C., Doree, M. and Karsenti, E. (1990). Regulation of microtubule dynamics by cdc2 protein-kinase in cell-free-extracts of xenopus eggs. *Nature* **343**, 233-238.

Verni, F., Somma, M. P., Gunsalus, K. C., Bonaccorsi, S., Belloni, B., Goldberg, M. L. and Gatti, M. (2004). Feo, the *Drosophila* homolog of PRC1, is required for central-spindle formation and cytokinesis. *Curr. Biol*. **14**, 1569-1575.

Weingartner, M., Binarova, P., Drykova, D., Schweighofer, A., David, J.-P., Heberle-Bors, E., Doonan, J. and Bögre, L. (2001). Dynamic recruitment of Cdc2 to specific microtubule structures during mitosis. *Plant Cell* **13**, 1929-1943.

Weingartner, M., Criqui, M.-C., Meszaros, T., Binarova, P., Schmit, A.-C., Helfer, A., Derevier, A., Erhardt, M., Bögre, L. and Genschik, P. (2004). Expression of a nondegradable cyclin B1 affects plant development and leads to endomitosis by inhibiting the formation of a phragmoplast. *Plant Cell* **16**, 643-657.

Wicker-Planquart, C., Stoppin-Mellet, V., Blanchoin, L. and Vantard, M. (2004). Interactions of tobacco microtubule-associated protein MAP65-1b with microtubules. *Plant J.* **39**, 126-134.

Zhu, C. and Jiang, W. (2005). Cell cycle-dependent translocation of PRC1 on the spindle by Kif4 is essential for midzone formation and cytokinesis. *Proc. Natl. Acad. Sci. USA* **102**, 343-348.

Journal of Cell Science